Article

Current Biology

Ecological Advantages and Evolutionary Limitations of Aggregative Multicellular Development

Graphical Abstract

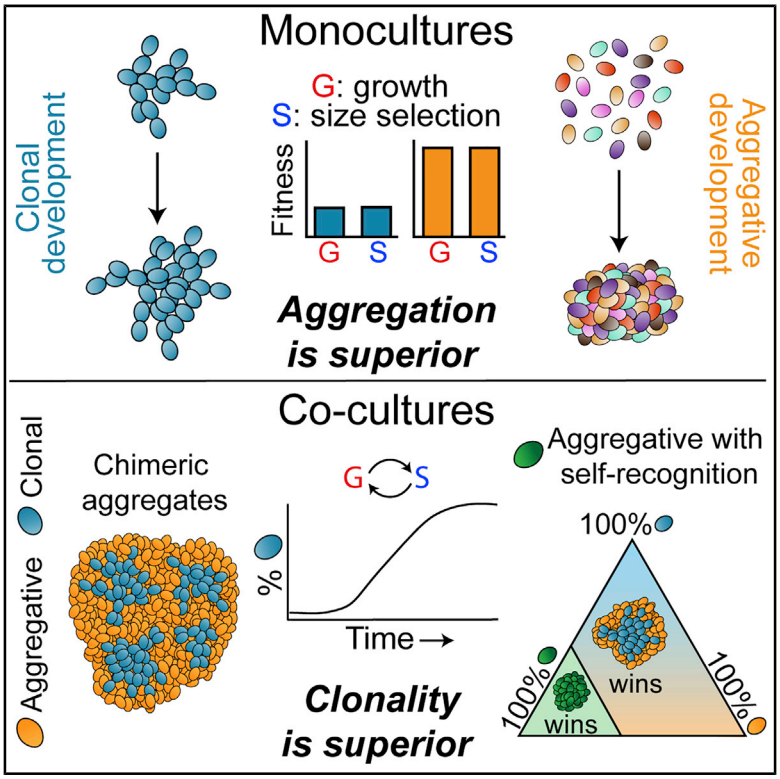

Authors

Jennifer T. Pentz, Pedro Márquez-Zacarías, G. Ozan Bozdag, Anthony Burnetti, Peter J. Yunker, Eric Libby, William C. Ratcliff

Correspondence

will.ratcliff@biology.gatech.edu

In Brief

Pentz et al. use yeast to examine the evolution of multicellular life cycles. Aggregative "floc" yeast have an ecological advantage in a fluctuating environment but are exploited by clonal "snowflake" yeast. Modeling suggests that such conflict may be unavoidable in aggregative organisms, helping explain their limited multicellular complexity.

Highlights

- In yeast, we show that aggregation is ecologically superior to clonal development
- Aggregative yeast, which bind permissively, were exploited by clonal yeast
- We show mathematically the benefits of aggregation require weak kin discrimination
- As a consequence, aggregative organisms can face persistent evolutionary conflict

Pentz et al., 2020, Current Biology *30*, 4155–4164
November 2, 2020
https://doi.org/10.1016/j.cub.2020.08.006

CellPress

Current Biology

CellPress

Article

Ecological Advantages and Evolutionary Limitations of Aggregative Multicellular Development

Jennifer T. Pentz,[1,2] Pedro Márquez-Zacarías,[2,3] G. Ozan Bozdag,[2] Anthony Burnetti,[2] Peter J. Yunker,[4] Eric Libby,[5] and William C. Ratcliff[2,6,*]

[1]Department of Molecular Biology, Umeå University, Umeå 90187, Sweden
[2]School of Biological Sciences, Georgia Institute of Technology, Atlanta, GA 30332, USA
[3]Interdisciplinary Graduate Program in Quantitative Biosciences, Georgia Institute of Technology, Atlanta, GA 30332, USA
[4]School of Physics, Georgia Institute of Technology, Atlanta, GA 30332, USA
[5]Department of Mathematics and Mathematical Statistics, Umeå University, Umeå 90187, Sweden
[6]Lead Contact
*Correspondence: will.ratcliff@biology.gatech.edu
https://doi.org/10.1016/j.cub.2020.08.006

SUMMARY

All multicellular organisms develop through one of two basic routes: they either aggregate from free-living cells, creating potentially chimeric multicellular collectives, or they develop clonally via mother-daughter cellular adhesion. Although evolutionary theory makes clear predictions about trade-offs between these developmental modes, these have never been experimentally tested in otherwise genetically identical organisms. We engineered unicellular baker's yeast (*Saccharomyces cerevisiae*) to develop either clonally ("snowflake"; Δ*ace2*) or aggregatively ("floc"; GAL1p::FLO1) and examined their fitness in a fluctuating environment characterized by periods of growth and selection for rapid sedimentation. When cultured independently, aggregation was far superior to clonal development, providing a 35% advantage during growth and a 2.5-fold advantage during settling selection. Yet when competed directly, clonally developing snowflake yeast rapidly displaced aggregative floc. This was due to unexpected social exploitation: snowflake yeast, which do not produce adhesive FLO1, nonetheless become incorporated into flocs at a higher frequency than floc cells themselves. Populations of chimeric clusters settle much faster than floc alone, providing snowflake yeast with a fitness advantage during competition. Mathematical modeling suggests that such developmental cheating may be difficult to circumvent; hypothetical "choosy floc" that avoid exploitation by maintaining clonality pay an ecological cost when rare, often leading to their extinction. Our results highlight the conflict at the heart of aggregative development: non-specific cellular binding provides a strong ecological advantage—the ability to quickly form groups—but this very feature leads to its exploitation.

INTRODUCTION

The evolution of complex life on Earth has occurred through key steps, in which formerly autonomous organisms evolve to become integral parts of a larger, higher level organism [1–5]. These have been termed major transitions in evolution [5] or evolutionary transitions in individuality [2, 6], one example of which is the transition from uni- to multicellularity. Multicellularity has evolved at least 25 times in organisms as diverse as bacteria [7, 8], archaea [9], and among deeply divergent lineages of eukaryotes [10, 11].

There are two basic modes of multicellular development. Cells can "stay together" after mitotic division, resulting in clonal development if the life cycle includes a genetic bottleneck [7, 12]. Alternatively, potentially unrelated cells can "come together" via aggregation, which occurs in a few groups of terrestrial micro-organisms [13, 14]. Clonal development is thought to possess several advantages over aggregation for multicellular construction. First, under clonal development, cells comprising the multicellular organism have a high degree of genetic relatedness [15], which aligns the fitness interests of individual cells, facilitating the evolution of cooperative traits (e.g., division of labor). Additionally, clonal development limits the potential for evolutionary conflict, as there is little standing genetic variation within an organism for selection to act on [16–19]. Through the same mechanism, clonal development stifles opportunities for the evolution of parasitic cell lineages that infiltrate and exploit functional organisms [20]. Second, organismal clonality facilitates cluster-level selection. Genetic uniformity among the cells in a group results in a direct correspondence between emergent multicellular traits and heritable information (primarily genes) responsible for generating these traits [21, 22]. Variation in the identity and frequency of different genotypes of cells within aggregates across multicellular generations undermines the heritability of emergent multicellular traits. Further, clonal development facilitates the shift from selection acting among cells to whole groups, simultaneously minimizing within-group genetic variation (thus largely preventing within-group selection) and maximizing between-group genetic variation [16]. Perhaps because of these benefits, the majority of independently evolved multicellular lineages develop clonally.

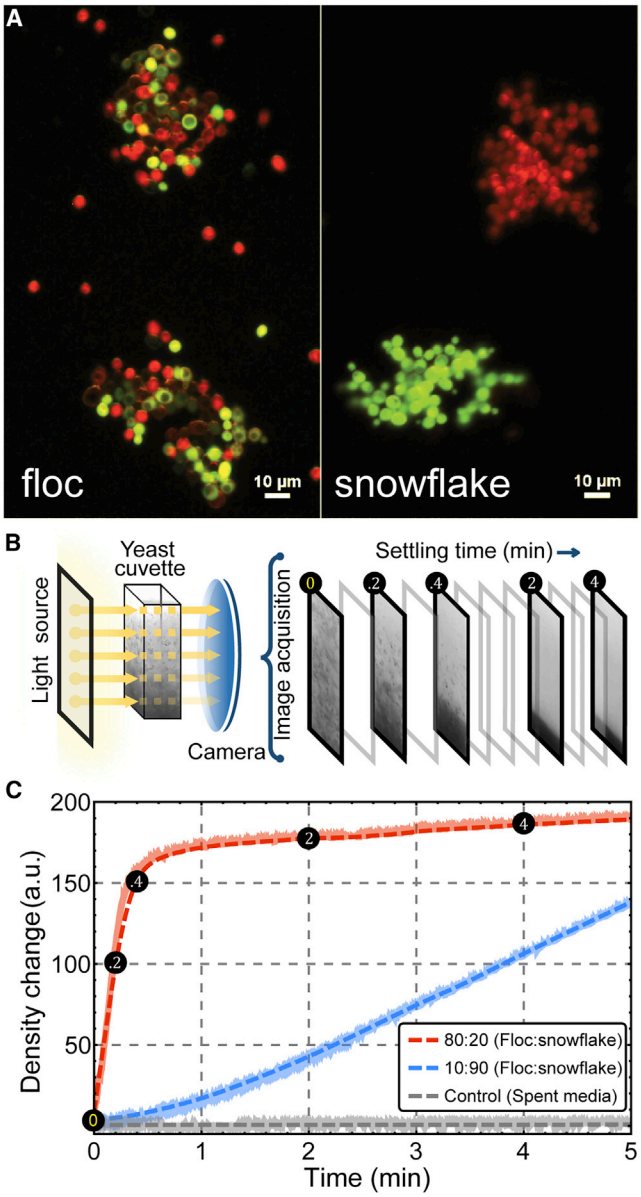

Figure 1. Synthetic Yeast System to Study Clonal and Aggregative Multicellular Development

(A) Synthetically created floc and snowflake yeast (*FLO1* insert and *ace2* knockout, respectively) labeled with either a red or green fluorescent marker. Both strains were created from the same unicellular ancestor. Flocs may be genetically diverse, although snowflake yeast form clonal clusters.

(B) Settling rate was measured using high-resolution video acquisition of back-illuminated yeast cultures over 5 min of settling. Individual pixel intensities, which correlate to yeast density, were used to measure the rate of density change (see Video S1).

(C) At every frame of the video, we calculated the density of each pixel within the cuvette. We measured the overall density change of the cuvette as the sum of individual pixel density changes. Raw density data (shadowed lines) were smoothed with a Savitzky-Golay smoothing function (dashed line), and the maximum slope of these dynamics is calculated as the settling rate. Shown are the density dynamics of fast (80:20 floc:snowflake) and slow (10:90 floc:snowflake) co-cultures, as well as a cell-free control where no density change is expected.

See also Video S1, Figure S6, and STAR Methods for technical details.

Yet aggregative development possesses a unique (but largely unappreciated) advantage: multicellular bodies can form far more rapidly [12]. If a group is formed via the staying together of cells after division, then its formation occurs by growth, causing the time required for body formation to scale with cellular generation time and organism size. In contrast, aggregation can occur far more rapidly. For example, aggregation of *Dictyostelium* into a multicellular mound can occur just 4–6 h after starvation [23], and flocculation of yeast can occur in seconds [24]. Indeed, aggregative development is common in organisms that rapidly switch from unicellular to multicellular life history strategies upon sudden environmental change (e.g., starvation in *Dictyostelium discoideum* [25] and *Myxococcus xanthus* [26]). Aggregation may also bring together cells with complementary properties, taking advantage of mutualistic interactions [27–31], but the evolutionary stability of this interaction generally requires a mechanism to limit social exploitation, such as a structured environment [31–34], host sanctions [35, 36], or partner fidelity across generations [37].

The origin of complex life cannot be understood in the absence of evolutionary mechanisms. It thus is imperative that we understand how basic mechanisms of multicellular development effect the subsequent evolution of multicellular complexity. Mathematical modeling [12, 19, 21, 22, 38–42] and experiments in diverse systems [20, 43–47] have generated consistent and robust predictions for the evolutionary consequences of variation in developmental mode. Yet, because no model organisms develop through both routes, no experiments have directly compared ecological versus evolutionary trade-offs between aggregative and clonal development. Here, we circumvent this historical limitation by engineering unicellular yeast (*Saccharomyces cerevisiae*) so that they form multicellular groups via either clonal development or aggregation.

The yeast *S. cerevisiae* can aggregate to form large clumps consisting of thousands of cells termed "flocs." Aggregation occurs via a lectin-like bonding between cell-surface FLO proteins and cell wall sugars in adjacent cells [44, 48]. Flocs preferentially form among mutual FLO^+ cells; FLO^- cells tend to be excluded from the group [49]. However, genetically diverse strains can join a floc if they are FLO^+ (Figure 1A). In contrast, "snowflake yeast" develop clonally, forming multicellular groups as a consequence of failed septum degradation after cytokinesis [50] (Figure 1A). When a cell-cell connection is severed, the group produces a viable propagule. This propagule experiences a single-cell genetic (but not physiological) bottleneck, as the most basal cell in the propagule is the mitotic parent of every cell in the group [50].

We engineered isogenic floc and snowflake yeast from a common unicellular ancestor and grew them in an environment that favors a rapid transition from unicellularity to multicellularity. Specifically, yeast were cultured with 24 h of shaking incubation, which selects for high growth rates, followed by selection for rapid sedimentation, which favors fast-settling groups. Aggregation was a superior strategy in monocultures: floc yeast, which spend most of the growth phase as unicells or small groups, grew 35% faster than snowflake yeast and rapidly formed large flocs during settling selection, settling 2.5 times as fast as snowflake yeast. Yet, in competition, snowflake yeast rapidly outcompete floc, the result of an unexpected social interaction. Despite

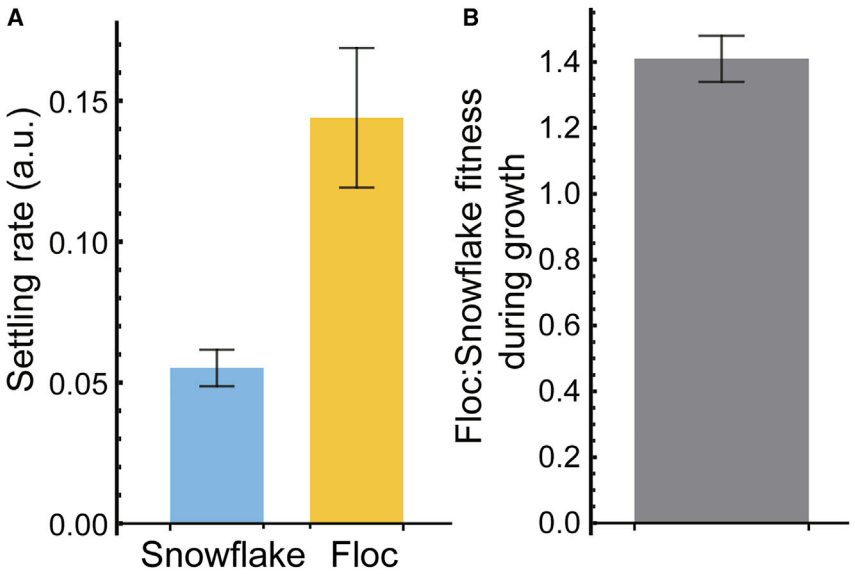

Figure 2. Aggregative Floc Yeast Are More Fit Than Clonally Developing Snowflake Yeast in an Environment Favoring Rapid Group Formation

Floc yeast are superior in two important life history traits that affect fitness in our experimental system. (A) Floc yeast settle 2.5 times faster than snowflake yeast (t_8 = 9.82; p < 0.0001; two-tailed t test). Error bars are the standard deviation of the mean (n = 8). (B) Floc yeast outcompete snowflake yeast over one 24-h growth period. Fitness was measured as the ratio of Malthusian growth parameters [55] for one 24-h period. The error bar is the standard deviation of the mean (n = 5).
See also Video S2.

being FLO$^-$, snowflake yeast embed themselves within floc clusters, making up a disproportionately high fraction of the biomass within flocs. Spatial analysis of chimeric aggregates demonstrates that snowflake yeast are uniformly, not randomly, distributed within the floc, suggesting a simple physical interaction between floc and snowflake is necessary for the formation of chimeric aggregate clusters. In principle, this parasitism could be prevented if floc evolved a partner choice mechanism, excluding heterospecific genotypes. We examined the invasion of such a "choosy" floc genotype using mathematical modeling. In our model, selective binding is ecologically costly, as there is an advantage for individual cells to form groups with as many other cells as possible (this way they form the largest groups). Rare choosy floc is therefore unable to invade permissive floc, snowflake yeast, or a population consisting of both. Because choosy floc's aggregative performance is strongly frequency dependent, it should perform poorly (relative to a permissive floc) in genetically diverse populations. This ecological cost may limit the evolution of strong kin recognition during aggregative development, paving the way for persistent evolutionary conflict.

RESULTS

There are two important life history traits that affect fitness in our fluctuating environment: growth during 24-h batch culture and settling rate during settling selection [51–53]. To measure settling rate, we developed a novel method to quantify the dynamical effects of aggregation and settling in real time (Figures 1B and 1C; Video S1; see STAR Methods section for details). Floc yeast are superior in both traits. First, floc yeast settle 2.5 times faster than snowflake yeast, rapidly forming large aggregates during settling selection (Figure 2A; Video S2; t_8 = 9.82; p < 0.0001; two-tailed t test). In direct competition, floc yeast outcompete snowflake yeast over one 24-h growth cycle (Figure 2B). This is likely a consequence of nutrient and oxygen limitation in snowflake clusters, which, in contrast to floc yeast, are always multicellular. To exclude the possibility that elevated rates of cell death in engineered snowflake yeast [51] may be contributing to differential fitness during growth, we measured the percentage of dead cells during stationary phase of floc and snowflake yeast. Both strains displayed similar rates of cell death (Figure S6C; p = 0.18; two-tailed t test). This is consistent with previous work showing that experimentally evolved snowflake yeast with loss-of-function mutations in *ace2* had apoptosis rates similar to that of the ancestor [54].

Co-culturing floc and snowflake yeast introduced markedly different behaviors. The settling rates of mixed populations increased dramatically (Figure 3A) and was highest when snowflake yeast were at an intermediate frequency (20%–50%; $F_{10,33}$ = 25.5; p < 0.0001; ANOVA, pairwise differences assessed with Tukey's honestly significant difference [HSD] with α = 0.05). To examine the effects of co-culture on fitness, we performed a series of competition experiments (two rounds of growth and settling) across a range of starting snowflake frequencies, from 1% to 99%, as determined by the ratio of initial inoculum volume given that both strains grow to similar final cell densities at stationary phase. Surprisingly, snowflake yeast were more fit than floc in all competitions, and their fitness was highly frequency dependent. When snowflake yeast were rare (starting at 1% of the initial culture inoculum), they had a small competitive advantage over floc (Figure 3B). This increased dramatically when they were slightly more common (10%–20% of initial culture inoculum) and then declined until snowflake yeast reached 80%. Flocculation was impeded when snowflake yeast constituted >80% of the population, allowing multicellular snowflake yeast to compete against largely unicellular floc, causing their relative fitness to again increase dramatically (Figures 3B and 3D). These dynamics appear to be the result of an unexpected interaction: when mixed together, snowflake yeast and floc form chimeric clusters during the settling phase of the experiment (Figure 3C). However, snowflake and floc yeast possess similar fitness (competitive success of 1) when snowflake yeast are at 80% frequency, suggesting that snowflake yeast may not be able to fully displace floc over longer evolutionary timescales. To test this, we performed an invasion assay with snowflake yeast starting at 2.5% of the initial population. Snowflake yeast were not only capable of invading floc, they drove them extinct after 10 days of competition (Figure 3E).

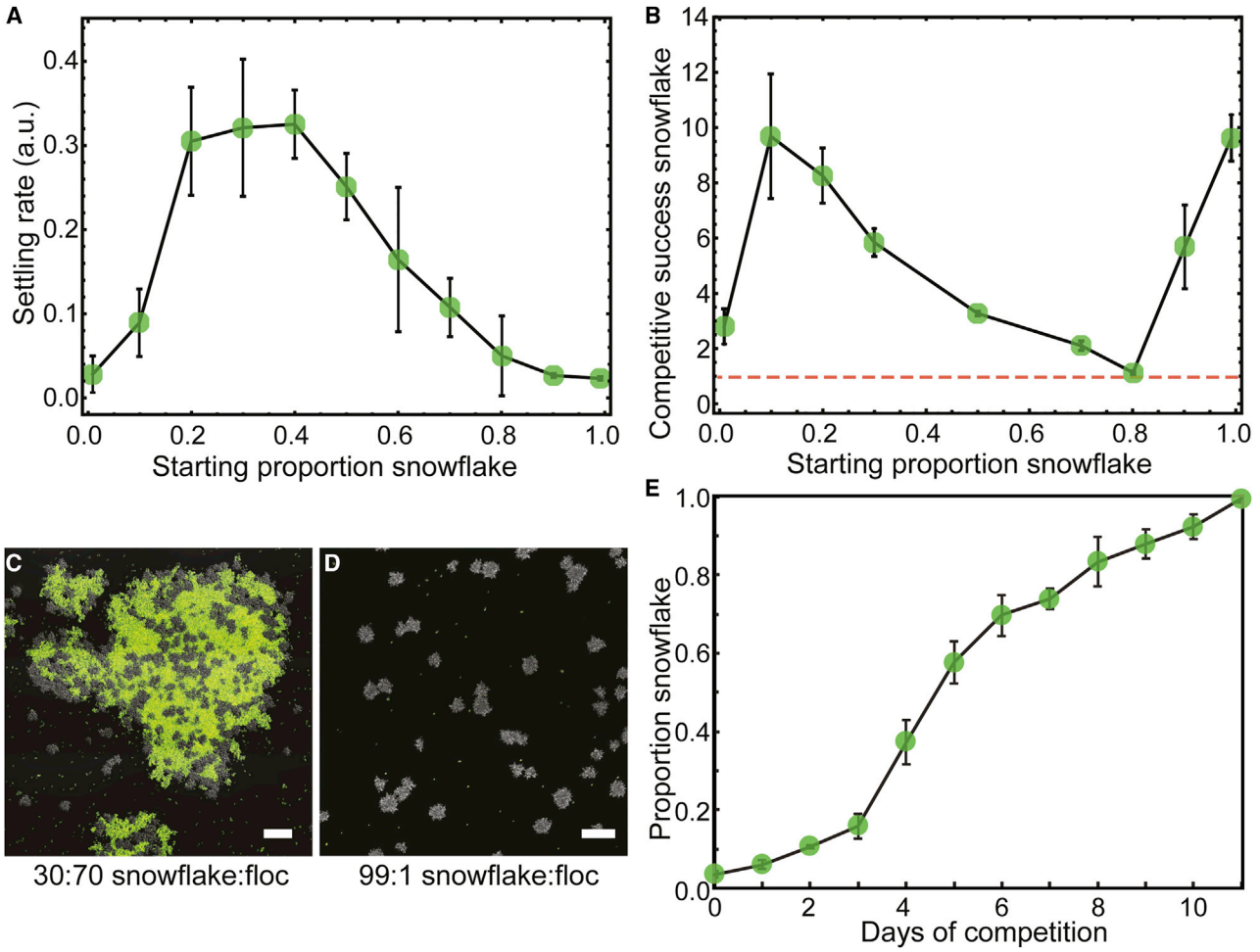

Figure 3. Co-culturing Floc and Snowflake Yeast

(A) Mixed populations settle more rapidly than snowflake yeast or floc alone. Settling occurs the most rapidly at intermediate frequencies (20%–50%; $F_{10,33}$ = 25.5; $p < 0.0001$; ANOVA followed by Tukey's HSD). Error bars are the standard deviation of four biological replicates; settling rate units are arbitrary.

(B) We measured the competitive success of snowflake yeast across two rounds of growth and settling. Snowflake yeast were more fit than floc at all genotype frequencies. Error bars are the standard deviation of five biological replicates.

(C and D) Snowflake yeast form chimeric aggregates with floc. Shown are snowflake yeast and GFP-tagged floc yeast starting at an initial inoculation ratio of 30:70 snowflake:floc-GFP (C) or 99:1 (D). Note that floc are below the concentration threshold required for aggregation, existing as unicells. Scale bars are 100 μm.

(E) Snowflake, starting at 2.5% population frequency, were able to fully displace floc over a 10-day competition experiment. Error bars are standard deviation of five biological replicates (n = 5).

To determine which phase of the periodic environmental regime (i.e., growth versus settling) favored snowflake yeast during competition with floc, we measured snowflake yeast competitive success across one culture cycle. Consistent with earlier experiments (Figure 2B), snowflake yeast lost to floc over one 24-h growth cycle (Figure 4). Snowflake yeast fitness during growth was negative frequency dependent ($y = -0.005x + 0.91$; $p < 0.0001$; linear regression). This is likely a consequence of overall nutrient consumption rates within our populations. When slower growing snowflake yeast make up a larger fraction of the population, they consume resources less quickly, extending the time over which their floc competitors can compound their growth rate advantage. In contrast to growth, however, snowflake yeast possessed an advantage during settling selection (Figure 4).

One way that snowflake yeast could gain an advantage during settling selection is if they are overrepresented in large, fast-settling chimeric aggregates. This would be unexpected, as *FLO1* yeast preferentially adhere to other floc cells, efficiently excluding non-flocculating unicells from flocs [49] (Figure S1A). We imaged co-cultures in which snowflake yeast were either rare (20% initial culture inoculum; Figure 5A) or common (80% initial culture inoculum; Figure 5B). Surprisingly, snowflake yeast were overrepresented in chimeric flocs (i.e., groups larger than the largest individual snowflakes; Figure 5C) at both genotype frequencies (Figures 5A and 5B).

One feature of chimeric aggregates that stands out is the appearance of a relatively uniform distribution of snowflake yeast within the aggregate (Figure S1B). We rarely see large patches of pure floc cells and never see large patches of just snowflake

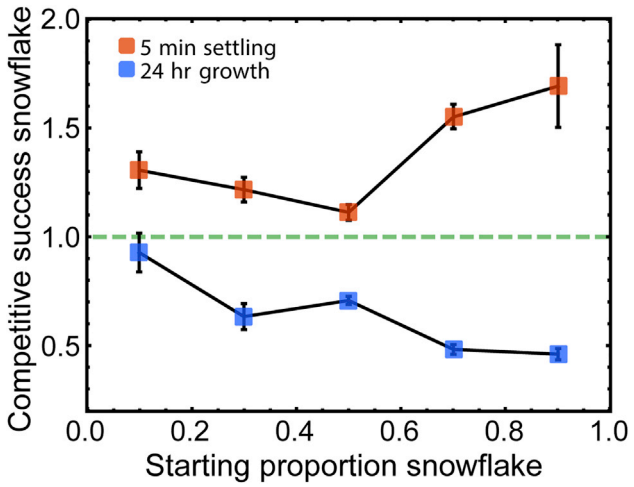

Figure 4. Snowflake Yeast Outcompete Floc during Settling Selection when Forming Chimeric Aggregates

We examined the competitive success of snowflake yeast in competition with floc during both growth (over 24 h of culture) and settling selection (5 min at 1 × *g*). Snowflake yeast had lower fitness at all starting genotype frequencies during the growth phase of the culture yet had higher fitness during settling selection. This is in stark contrast to what we observe in pure culture, where floc yeast settle 2.5 times as quickly as snowflakes (Figure 1B). Error bars are standard deviation of five biological replicates (n = 5).

yeast. To quantify the spatial distribution of snowflake yeast within chimeric aggregates, we first measured the spatial autocorrelation function (Moran's *I*). We found that the correlation length of snowflake cells is similar in size to the cluster radius (14.1 ± 0.2 μm, 14.2 ± 0.2 μm, 13.9 ± 0.1 μm, and 11.7 ± 1.3 μm for 30%, 20%, 10%, and 1% snowflake yeast, respectively), as expected. We next characterized the spatial distribution of whole snowflake clusters by calculating the pair correlation function, *g(r)*, which measures the probability of finding two whole clusters separated by a given distance (Figure S1C), normalized by a random distribution (measured between clusters, not among cells within snowflake yeast) at the same density. We find that the distribution of snowflake yeast clusters is highly structured within aggregates. Clusters are unlikely to be found very close to each other; specifically, clusters are less likely to be found with a center-to-center separation less than or equal to 1.3 times their diameter than expected if everything that collided during aggregation adhered. Relatedly, clusters are more likely to be found with center-to-center separations between 1.3 and 1.9 times their diameter than expected by chance. Thus, the distribution of clusters within an aggregate is more evenly dispersed than would be expected by a random mixing of genotypes. This even dispersal suggests that snowflake yeast are capable of binding to floc yeast, but not other snowflake yeast, during aggregate formation. Consistent with this hypothesis, floc yeast appear to act as an adhesive, binding together snowflakes (Figure S1D; we do not see any evidence of direct snowflake-snowflake adhesion). This analysis suggests a biomechanical mechanism for snowflake yeast's ability to invade flocs: snowflake yeast efficiently adhere to floc yeast, likely being coated by floc during aggregation and facilitating their ability to join floc aggregates.

A classic solution to social conflict in aggregating multicellular organisms is kin recognition, allowing individuals to avoid cheating by only cooperating with close relatives [56–59]. Here, we examine whether kin recognition would solve the cooperative dilemma faced by floc yeast by constructing a mathematical model (see STAR Methods). Briefly, we assume that there are three types of yeast: a snowflake yeast strain (*S*); a "choosy floc" (*C*) that uses a self-recognition mechanism to adhere just to clonemates; and a "permissive floc" (*P*) that has no such self-recognition mechanism, adhering to both permissive floc and snowflake yeast. We simplify our analysis by focusing strictly on the role of self-recognition in the formation of groups. Thus, we assume that, after some initial period of population growth, there is an aggregation phase in which cells stop reproducing and the flocculating yeast aggregate to form groups. Rather than modeling the complex dynamics of group size and shape during settling selection, we make the simplifying assumption that only the largest groups survive. Although floc yeast rapidly form groups, increasing in size as a function of time (Figures S2C and S2D), snowflakes themselves do not change in size (as there is no growth; Figures S2A and S2B), though they may join aggregates with permissive floc. When floc are growing at higher density, it takes less time to form groups that can outcompete snowflake yeast during settling selection (Figure S2C).

We consider all pairwise competitions between permissive floc, choosy floc, and snowflake yeast for different starting genotype frequencies (Figures 6A–6C). For each competition, we simulate the aggregation process and then select 10% of the population from the largest groups (selection that is roughly analogous to the experimental protocol). We find that snowflake yeast are overrepresented within large, fast-settling flocs (recapitulating our experimental data; Figure 6A), allowing them to outcompete permissive floc, regardless of their starting frequency. We also find that the largest chimeric aggregates, representing the fastest settling aggregates, form with intermediate frequencies of snowflake yeast (peaking at 40% *S*; Figure S2E). This is similar to our experimental data (Figure 3A), where the fastest settling aggregates are also found at intermediate frequencies (20%–50%). In contrast, if snowflake and choosy floc compete, then choosy floc increases in abundance whenever it constitutes the majority (specifically, more than ~60%; Figure 6B) of the population, though the precise frequency depends on model parameters, like density, aggregation time, and binding probability (Figures S3B, S3D, and S4F). Thus, neither snowflake yeast nor choosy floc can invade each other when rare. Finally, because permissive and choosy floc behave the same in the absence of snowflake yeast (they do not co-aggregate), their dynamics are positively frequency dependent and neither can invade from rare (Figures 6C, S3C, S3F, and S4E). We observed the same dynamics as in our deterministic model (Figure 6) using a stochastic approach (see Figure S5 and STAR Methods for details).

We see an interesting ecological interaction in our model: in a three-way competition, snowflakes can invade populations of choosy floc with the help of permissive floc (Figure 6D; see results from longer or shorter durations of aggregation in Figures S3G and S4G–S4I). By forming large, fast-settling chimeric aggregates, mixtures of snowflake and permissive floc gain an ecological advantage over choosy floc, outcompeting it

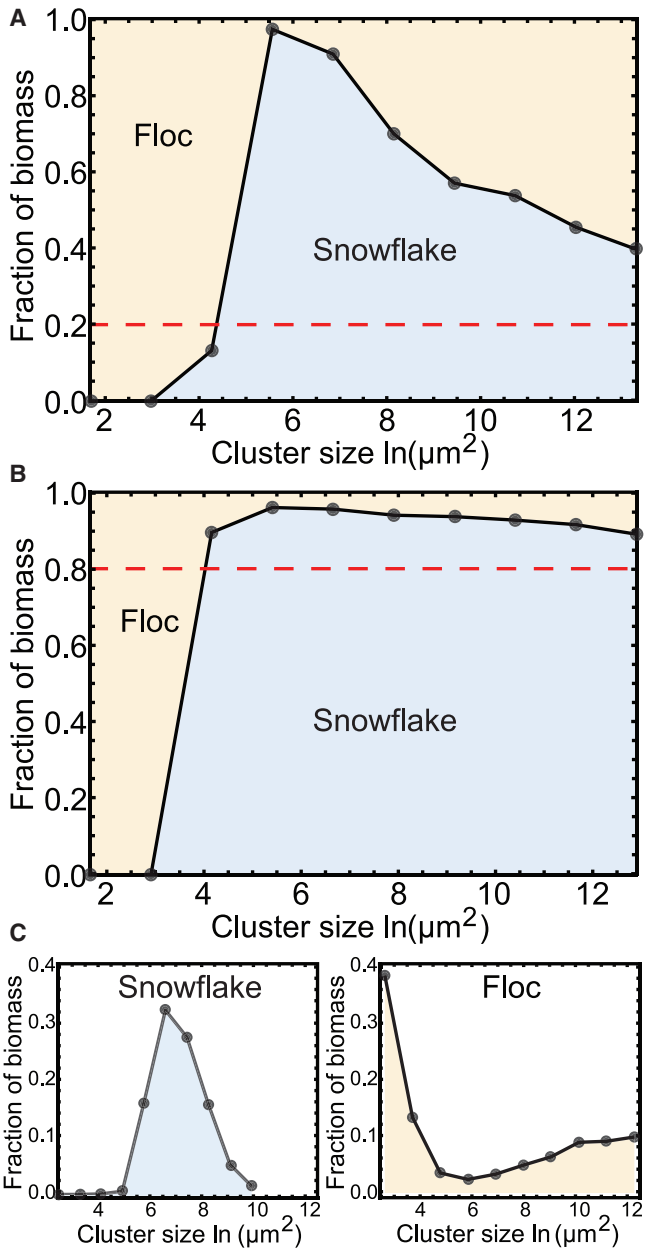

Figure 5. Snowflake Yeast Are Overrepresented in Large Chimeric Aggregates

(A and B) Snowflake yeast constitute a larger fraction of the biomass within large flocs than is expected by their overall population frequency (red dashed line). Shown are snowflake yeast at 20% (A) and 80% (B) overall frequency.
(C) Size distributions of pure snowflake and floc cultures.
See also Figure S1.

(Figure 6D). Of course, this is an unstable alliance, as snowflake yeast's exploitation of permissive floc will ultimately drive all aggregative strategies to extinction (Figures 6A, 6D, and S3H). Sometimes, however, this social exploitation of floc is costly for snowflake yeast. When snowflake and permissive floc are below the threshold required to displace choosy floc, exploitation of permissive floc results in a rapid deterioration of their ability to make large chimeric aggregates, to the detriment of both snowflake and permissive floc (Figures 6D and S3I). These results were not qualitatively changed by the inclusion of a growth phase in our model, in which floc cells had a 35% growth advantage to snowflake yeast (Figures 2B, S4J, and S4K).

A simple extrapolation of our model highlights the cost of kin discrimination during aggregative development. Consider a genetically diverse population of aggregative organisms, each of which only adheres to clonemates. Because aggregation rate is frequency and density dependent (Figures 6, S3, and S4), any genotypes that are locally rare will be unable to rapidly form large groups, as they will be capable of interacting with only a small fraction of the population. Strict kin recognition during aggregation therefore undermines the ecological advantage of aggregation upon its initial evolution, suppressing its origination. This is even more of a problem if the benefits of aggregation require that a size threshold be met (e.g., enough individuals to form a multicellular fruiting body) [60].

DISCUSSION

Development is a fundamental aspect of multicellularity, orchestrating the pattern of cellular behaviors that give rise to multicellular phenotype and influencing a lineage's evolutionary potential. Despite significant theoretical work, the lack of appropriate model systems has limited our ability to directly test the role of developmental mechanism on the subsequent evolution of multicellularity. We circumvent this limitation by engineering aggregative and clonal development from an isogenic unicellular yeast ancestor (Figure 1A).

We grew our yeast under conditions in which selection favored a rapid transition from a unicellular to multicellular stage, the type of environment that is thought to favor aggregative multicellularity [12]. The advantage that aggregative floc yeast showed in monoculture (Figure 2) evaporated once they were competed directly with clonally developing snowflake yeast (Figure 3), the result of a wholly unexpected social exploitation. Snowflake yeast, which do not produce adhesive Flo1 proteins, embed themselves within large floccy aggregates at a higher frequency than the floc genotype (Figures 3C, 3D, 5, and S1B–S1D). As a result of this social exploitation, snowflake yeast rapidly displace floc (Figures 3B and 3E). This result is even more striking in light of prior work in other yeast systems. First, Driscoll et al. [61] observed the evolution of a stable coexistence between unicellular and multicellular genotypes in *Kluyveromyces lactus* following selection for multicellularity, where unicellular yeast act as "free riders" that associate with fast-settling snowflake clusters via flocculation. Here, snowflake yeast act as the unrelated free riders, exploiting the benefits of rapid, non-specific aggregation in flocculating yeast but, rather than resulting in coexistence, are competitively dominant (Figure 3E). Second, Smukalla et al. [49] showed that *FLO1* acts as a greenbeard gene, excluding unicellular *FLO1*$^-$ competitors from the floc. This is thought to be a consequence of preferential binding between *FLO1*$^+$ cells, leading to phase separation. In our case, the ability for *FLO1*$^-$ snowflake yeast to co-aggregate with floc appears to arise as a consequence of their branchy structure, allowing them to become entangled within a floc. Our results also provide context for understanding the results of a prior experiment, in which five wild isolates of flocculating yeast were

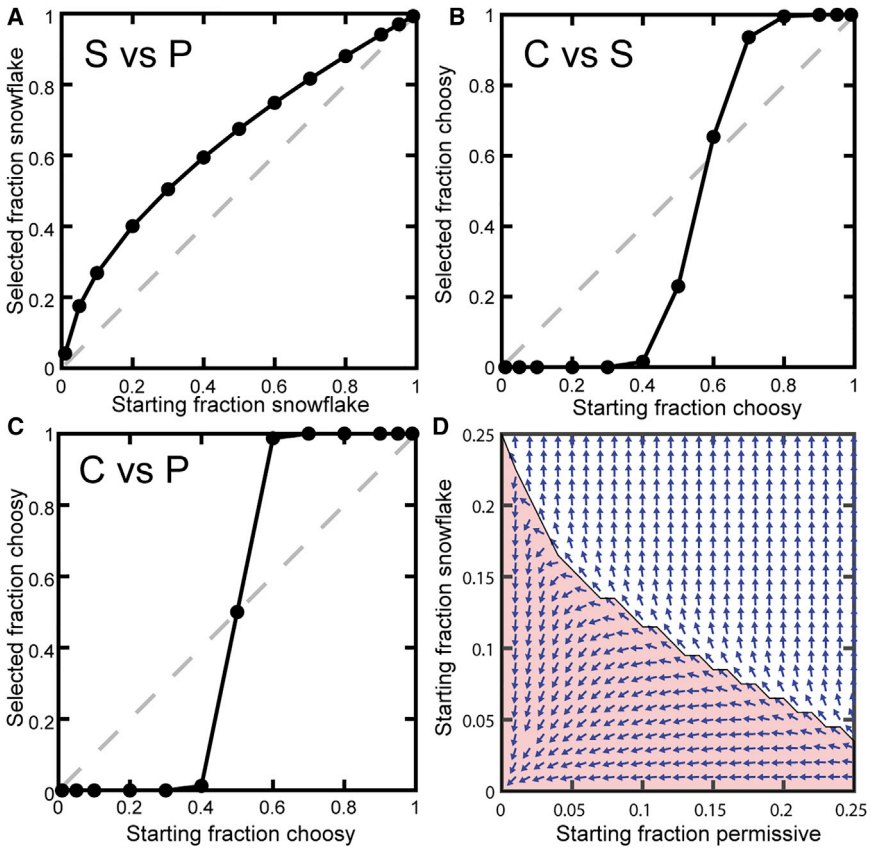

Figure 6. Modeling the Dynamics of Kin Recognition in Floc Yeast

(A) Snowflake yeast, *S*, were capable of displacing permissive floc, *P*, at all frequencies during aggregation and settling selection.

(B and C) In contrast, the fitness of choosy floc, *C*, in competition with snowflake yeast (B) and permissive floc (C) were positively frequency dependent.

(D) Phase portrait showing the changes in permissive floc and snowflake yeast after one round of settling selection in competition with choosy floc. Arrows show the direction of change in proportion of *S* and *P* as a function of different starting frequencies. Choosy floc were only able to increase in frequency (red shading) when they were common enough to rapidly find clonemates for aggregation.

See also Figures S2–S5.

evolved with daily settling selection. Here, snowflake yeast arose *de novo* and largely displaced their floc ancestors in 35/40 replicate populations [46].

Self/nonself recognition systems play a key role during the evolution of multicellularity, limiting the potential for within-organism genetic conflict [57, 58, 62]. This may be especially important in lineages that develop aggregatively, as they are more likely to form genetically diverse multicellular groups. Kin-recognition mechanisms have evolved independently in cellular slime molds [57, 62] and *Myxococcus* bacteria [58, 63], both of which develop via aggregation. We explored the evolution of self-recognition in our system using a mathematical model. We considered our standard permissive floc, which binds to other permissive floc or snowflake yeast, and a hypothetical choosy floc, which only attaches to clonemates. Although it might seem like choosy floc (which axiomatically cannot experience social conflict) would always be at an advantage, this was not true. Permissive binding increases opportunities for cell-cell adhesion, increasing aggregation speed and group size. Indeed, our experiments show striking support for this hypothesis: floc that formed chimeric aggregates were capable of settling much faster than floc alone (Figure 3A). In our model, choosy floc pay an ecological cost when rare, as they can only bind a small fraction of the cells in the population, forming small groups. This strong positive-frequency-dependent selection makes it difficult for strong kin recognition to arise from a population of permissive ancestors, a cost that is compounded if the population is composed of multiple choosy genotypes, each of which is only capable of adhering to clonemates.

Consistent with the hypothesis that the evolutionary benefits of strong kin discrimination may not be worth the ecological costs, kin discrimination systems in extant aggregative organisms are relatively permissive. Genetic diversity is often high at small spatial scales in both myxobacteria [58, 64] and slime molds [65–67], and wild-collected isolates readily form multi-clonal groups under laboratory conditions [58, 62, 65–67]. Allorecognition in both *D. discoideum* and myxobacteria are mediated by a single protein pair: TgrB1/TgrC1 [68, 69] and TraA/B [69, 70], respectively. Single-locus recognition systems face numerous challenges: first, the ability of a single locus to act as a proxy for genome-wide relatedness can be degraded by recombination, mutation, and horizontal gene transfer [71]. Once decoupled from either overall relatedness or genes underlying cooperative traits, a recognition system can no longer be used to drive positive assortment among cooperators. Second, selection acting on recognition-mediated cooperation tends to reduce the diversity in recognition alleles in the population, undermining the variation necessary to provide effective discrimination between cooperators and cheats [71] (i.e., Crozier's paradox) [72]. There is nothing in principle that would restrict aggregative organisms to single-locus recognition systems. Multilocus recognition systems are more robust and precise [71, 73] and are common in nature (e.g., in bacterial systems [74, 75]; unicellular protists, such as fungi and slime molds [76]; major histocompatibility complex [MHC] loci [77–79]; and self-incompatibility loci in outbreeding plants [80]), raising the possibility that permissive aggregation is in fact a desirable feature in an aggregative life cycle, not a yet-to-be-improved bug.

Our results highlight a fundamental trade-off faced during aggregative development: selection for rapid group formation often favors permissive binding, but the resulting

high within-group genetic diversity lays the foundation for persistent evolutionary conflict. This has important implications for the evolution of multicellular complexity, as the resulting genetic conflict can undermine multicellular adaptation [45]. Indeed, aggregation is relatively uncommon among independently evolved multicellular lineages [14, 81], and all known examples of independently evolved "complex multicellularity" (i.e., metazoans, land plants, mushroom-forming fungi, brown algae, and red algae) [11] develop clonally. In the context of major evolutionary transitions, aggregation appears to be self-limiting, the evolutionary potential of aggregative lineages constrained by an ecological imperative for effective group formation.

STAR★METHODS

Detailed methods are provided in the online version of this paper and include the following:

- KEY RESOURCES TABLE
- RESOURCE AVAILABILITY
  - Lead Contact
  - Materials Availability
  - Data and code availability
- EXPERIMENTAL MODEL AND SUBJECT DETAILS
- METHOD DETAILS
  - Measuring settling rate
  - Competitive success assay
  - Invasion from rare experiment
  - Competitive success during growth and settling
  - Examining aggregate composition
  - Mathematical modeling
  - Stochastic model
  - Direct measurement of settled biomass
  - Measuring the ratio of FLO+ and FLO- unicells in flocs
  - Measuring the frequency of dead cells
- QUANTIFICATION AND STATISTICAL ANALYSIS

SUPPLEMENTAL INFORMATION

Supplemental Information can be found online at https://doi.org/10.1016/j.cub.2020.08.006.

ACKNOWLEDGMENTS

We would like to thank Kevin Verstrepen for providing us with strain *S. cerevisiae* KV210, which contained the *GALp::FLO1* construct, and Daniel Weissman for insightful feedback on the manuscript. This work was supported by NSF DEB-1845363 to W.C.R., NSF grant no. IOS-1656549 to W.C.R. and P.J.Y., NSF grant no. IOS-1656849 to E.L., and a Packard Foundation Fellowship for Science and Engineering to W.C.R.

AUTHOR CONTRIBUTIONS

J.T.P., W.C.R., and P.M.-Z. designed the experiments. J.T.P. conducted the experiments. J.T.P. and P.M.-Z. designed the settling rate analysis pipeline. G.O.B. performed the 10-day floc/yeast competition experiment and measured percentage of cell death. E.L. performed the modeling. P.J.Y. performed the spatial analysis of snowflake yeast within chimeric aggregates. All authors contributed to data analysis and interpretation. J.T.P. and W.C.R. wrote the first draft of the paper, and all authors contributed to revision.

DECLARATION OF INTERESTS

The authors declare no competing interests.

Received: September 6, 2019
Revised: May 14, 2020
Accepted: August 3, 2020
Published: September 3, 2020

REFERENCES

1. Bonner, J.T. (1988). The Evolution of Complexity by Means of Natural Selection (Princeton University).
2. Buss, L.W. (2014). The Evolution of Individuality (Princeton University).
3. Leigh, E.G. (1977). How does selection reconcile individual advantage with the good of the group? Proc. Natl. Acad. Sci. USA *74*, 4542–4546.
4. Maynard Smith, J. (1988). Evolutionary progress and the levels of selection. In Evolutionary Progress, M.H. Nitecki, ed. (University of Chicago Press), pp. 219–230.
5. Szathmáry, E., and Smith, J.M. (1997). Major Transitions in Evolution (Oxford University).
6. Michod, R.E. (2007). Evolution of individuality during the transition from unicellular to multicellular life. Proc. Natl. Acad. Sci. USA *104* (*Suppl 1*), 8613–8618.
7. Bonner, J.T. (1998). The origins of multicellularity. Integr. Biol. Issues News Rev. *1*, 27–36.
8. Kaiser, D. (2001). Building a multicellular organism. Annu. Rev. Genet. *35*, 103–123.
9. Robinson, R.W. (1986). Life cycles in the methanogenic archaebacterium Methanosarcina mazei. Appl. Environ. Microbiol. *52*, 17–27.
10. Grosberg, R.K., and Strathmann, R.R. (2007). The evolution of multicellularity: a minor major transition? Annu. Rev. Ecol. Evol. Syst. *38*, 621–654.
11. Knoll, A.H. (2011). The multiple origins of complex multicellularity. Annu. Rev. Earth Planet. Sci. *39*, 217–239.
12. Tarnita, C.E., Taubes, C.H., and Nowak, M.A. (2013). Evolutionary construction by staying together and coming together. J. Theor. Biol. *320*, 10–22.
13. Bonner, J.T. (2000). First Signals: The Evolution of Multicellular Development (Princeton University).
14. Du, Q., Kawabe, Y., Schilde, C., Chen, Z.H., and Schaap, P. (2015). The evolution of aggregative multicellularity and cell–cell communication in the Dictyostelia. J. Mol. Biol. *427*, 3722–3733.
15. Fisher, R.M., Cornwallis, C.K., and West, S.A. (2013). Group formation, relatedness, and the evolution of multicellularity. Curr. Biol. *23*, 1120–1125.
16. Grosberg, R.K., and Strathmann, R.R. (1998). One cell, two cell, red cell, blue cell: the persistence of a unicellular stage in multicellular life histories. Trends Ecol. Evol. *13*, 112–116.
17. Hamilton, W.D. (1964). The genetical evolution of social behaviour. II. J. Theor. Biol. *7*, 17–52.
18. Michod, R.E. (2005). On the transfer of fitness from the cell to the multicellular organism. Biol. Philos. *20*, 967–987.
19. Michod, R.E., and Roze, D. (2001). Cooperation and conflict in the evolution of multicellularity. Heredity *86*, 1–7.
20. Queller, D.C. (2000). Relatedness and the fraternal major transitions. Philos. Trans. R. Soc. Lond. B Biol. Sci. *355*, 1647–1655.
21. Ratcliff, W.C., Herron, M., Conlin, P.L., and Libby, E. (2017). Nascent life cycles and the emergence of higher-level individuality. Philos. Trans. R. Soc. Lond. B Biol. Sci. *372*, 20160420.
22. Libby, E., and B Rainey, P. (2013). A conceptual framework for the evolutionary origins of multicellularity. Phys. Biol. *10*, 035001.
23. Chisholm, R.L., and Firtel, R.A. (2004). Insights into morphogenesis from a simple developmental system. Nat. Rev. Mol. Cell Biol. *5*, 531–541.

24. Stratford, M., and Keenan, M.H. (1988). Yeast flocculation: quantification. Yeast *4*, 107–115.

25. Bonner, J.T. (1967). The Cellular Slime Moulds, Second Edition (Princeton University).

26. Kaiser, D., Manoil, C., and Dworkin, M. (1979). Myxobacteria: cell interactions, genetics, and development. Annu. Rev. Microbiol. *33*, 595–639.

27. Ispolatov, I., Ackermann, M., and Doebeli, M. (2012). Division of labour and the evolution of multicellularity. Proc. Biol. Sci. *279*, 1768–1776.

28. Boles, B.R., Thoendel, M., and Singh, P.K. (2004). Self-generated diversity produces "insurance effects" in biofilm communities. Proc. Natl. Acad. Sci. USA *101*, 16630–16635.

29. Pande, S., and Velicer, G.J. (2018). Chimeric synergy in natural social groups of a cooperative microbe. Curr. Biol. *28*, 487.

30. van Gestel, J., Vlamakis, H., and Kolter, R. (2015). From cell differentiation to cell collectives: Bacillus subtilis uses division of labor to migrate. PLoS Biol. *13*, e1002141.

31. Pande, S., Kaftan, F., Lang, S., Svatoš, A., Germerodt, S., and Kost, C. (2016). Privatization of cooperative benefits stabilizes mutualistic cross-feeding interactions in spatially structured environments. ISME J. *10*, 1413–1423.

32. Shou, W., Ram, S., and Vilar, J.M. (2007). Synthetic cooperation in engineered yeast populations. Proc. Natl. Acad. Sci. USA *104*, 1877–1882.

33. Kim, H.J., Boedicker, J.Q., Choi, J.W., and Ismagilov, R.F. (2008). Defined spatial structure stabilizes a synthetic multispecies bacterial community. Proc. Natl. Acad. Sci. USA *105*, 18188–18193.

34. Van Dyken, J.D., Müller, M.J., Mack, K.M., and Desai, M.M. (2013). Spatial population expansion promotes the evolution of cooperation in an experimental Prisoner's Dilemma. Curr. Biol. *23*, 919–923.

35. Visick, K.L., Foster, J., Doino, J., McFall-Ngai, M., and Ruby, E.G. (2000). Vibrio fischeri lux genes play an important role in colonization and development of the host light organ. J. Bacteriol. *182*, 4578–4586.

36. Kiers, E.T., Rousseau, R.A., West, S.A., and Denison, R.F. (2003). Host sanctions and the legume-rhizobium mutualism. Nature *425*, 78–81.

37. Bright, M., and Bulgheresi, S. (2010). A complex journey: transmission of microbial symbionts. Nat. Rev. Microbiol. *8*, 218–230.

38. De Monte, S., and Rainey, P.B. (2014). Nascent multicellular life and the emergence of individuality. J. Biosci. *39*, 237–248.

39. Amado, A., Batista, C., and Campos, P.R.A. (2018). A theoretical approach to the size-complexity rule. Evolution *72*, 18–29.

40. Garcia, T., Doulcier, G., and De Monte, S. (2015). The evolution of adhesiveness as a social adaptation. eLife *4*, e08595.

41. Biernaskie, J.M., and West, S.A. (2015). Cooperation, clumping and the evolution of multicellularity. Proc. Biol. Sci. *282*, 20151075.

42. Staps, M., van Gestel, J., and Tarnita, C.E. (2019). Emergence of diverse life cycles and life histories at the origin of multicellularity. Nat. Ecol. Evol. *3*, 1197–1205.

43. Bastiaans, E., Debets, A.J., and Aanen, D.K. (2016). Experimental evolution reveals that high relatedness protects multicellular cooperation from cheaters. Nat. Commun. *7*, 11435.

44. Brückner, S., and Mösch, H.-U. (2012). Choosing the right lifestyle: adhesion and development in Saccharomyces cerevisiae. FEMS Microbiol. Rev. *36*, 25–58.

45. Kuzdzal-Fick, J.J., Fox, S.A., Strassmann, J.E., and Queller, D.C. (2011). High relatedness is necessary and sufficient to maintain multicellularity in Dictyostelium. Science *334*, 1548–1551.

46. Pentz, J.T., Travisano, M., and Ratcliff, W.C. (2014). Clonal development is evolutionarily superior to aggregation in wild-collected Saccharomyces cerevisiae. Artif. Life Conf. Proc. *26*, 550–554.

47. Hammerschmidt, K., Rose, C.J., Kerr, B., and Rainey, P.B. (2014). Life cycles, fitness decoupling and the evolution of multicellularity. Nature *515*, 75–79.

48. Guo, B., Styles, C.A., Feng, Q., and Fink, G.R. (2000). A Saccharomyces gene family involved in invasive growth, cell-cell adhesion, and mating. Proc. Natl. Acad. Sci. USA *97*, 12158–12163.

49. Smukalla, S., Caldara, M., Pochet, N., Beauvais, A., Guadagnini, S., Yan, C., Vinces, M.D., Jansen, A., Prevost, M.C., Latgé, J.-P., et al. (2008). FLO1 is a variable green beard gene that drives biofilm-like cooperation in budding yeast. Cell *135*, 726–737.

50. Ratcliff, W.C., Fankhauser, J.D., Rogers, D.W., Greig, D., and Travisano, M. (2015). Origins of multicellular evolvability in snowflake yeast. Nat. Commun. *6*, 6102.

51. Ratcliff, W.C., Denison, R.F., Borrello, M., and Travisano, M. (2012). Experimental evolution of multicellularity. Proc. Natl. Acad. Sci. USA *109*, 1595–1600.

52. Ratcliff, W.C., Pentz, J.T., and Travisano, M. (2013). Tempo and mode of multicellular adaptation in experimentally evolved Saccharomyces cerevisiae. Evolution *67*, 1573–1581.

53. Conlin, P.L., and Ratcliff, W.C. (2016). Trade-offs drive the evolution of increased complexity in nascent multicellular digital organisms. In Multicellularity: Origins and Evolution, K.J. Niklas, and S.A. Newman, eds. (MIT), pp. 131–147.

54. Pentz, J.T., Taylor, B.P., and Ratcliff, W.C. (2016). Apoptosis in snowflake yeast: novel trait, or side effect of toxic waste? J. R. Soc. Interface *13*, 20160121.

55. Lenski, R.E., Rose, M.R., Simpson, S.C., and Tadler, S.C. (1991). Long-term experimental evolution in Escherichia coli. I. Adaptation and divergence during 2,000 generations. Am. Nat. *138*, 1315–1341.

56. Strassmann, J.E., Gilbert, O.M., and Queller, D.C. (2011). Kin discrimination and cooperation in microbes. Annu. Rev. Microbiol. *65*, 349–367.

57. Kalla, S.E., Queller, D.C., Lasagni, A., and Strassmann, J.E. (2011). Kin discrimination and possible cryptic species in the social amoeba Polysphondylium violaceum. BMC Evol. Biol. *11*, 31.

58. Vos, M., and Velicer, G.J. (2009). Social conflict in centimeter-and global-scale populations of the bacterium Myxococcus xanthus. Curr. Biol. *19*, 1763–1767.

59. Stefanic, P., Kraigher, B., Lyons, N.A., Kolter, R., and Mandic-Mulec, I. (2015). Kin discrimination between sympatric Bacillus subtilis isolates. Proc. Natl. Acad. Sci. USA *112*, 14042–14047.

60. Kim, S.K., and Kaiser, D. (1991). C-factor has distinct aggregation and sporulation thresholds during Myxococcus development. J. Bacteriol. *173*, 1722–1728.

61. Driscoll, W.W., and Travisano, M. (2017). Synergistic cooperation promotes multicellular performance and unicellular free-rider persistence. Nat. Commun. *8*, 15707.

62. Ostrowski, E.A., Katoh, M., Shaulsky, G., Queller, D.C., and Strassmann, J.E. (2008). Kin discrimination increases with genetic distance in a social amoeba. PLoS Biol. *6*, e287.

63. Rendueles, O., Zee, P.C., Dinkelacker, I., Amherd, M., Wielgoss, S., and Velicer, G.J. (2015). Rapid and widespread de novo evolution of kin discrimination. Proc. Natl. Acad. Sci. USA *112*, 9076–9081.

64. Vos, M., and Velicer, G.J. (2006). Genetic population structure of the soil bacterium Myxococcus xanthus at the centimeter scale. Appl. Environ. Microbiol. *72*, 3615–3625.

65. Fortunato, A., Strassmann, J.E., Santorelli, L., and Queller, D.C. (2003). Co-occurrence in nature of different clones of the social amoeba, Dictyostelium discoideum. Mol. Ecol. *12*, 1031–1038.

66. Sathe, S., Kaushik, S., Lalremruata, A., Aggarwal, R.K., Cavender, J.C., and Nanjundiah, V. (2010). Genetic heterogeneity in wild isolates of cellular slime mold social groups. Microb. Ecol. *60*, 137–148.

67. Kaushik, S., and Nanjundiah, V. (2003). Evolutionary questions raised by cellular slime mould development. Proc. Indian Natn. Sci. Acad. B *69*, 825–852.

68. Hirose, S., Santhanam, B., Katoh-Kurosawa, M., Shaulsky, G., and Kuspa, A. (2015). Allorecognition, via TgrB1 and TgrC1, mediates the transition

from unicellularity to multicellularity in the social amoeba Dictyostelium discoideum. Development *142*, 3561–3570.

69. Pathak, D.T., Wei, X., Dey, A., and Wall, D. (2013). Molecular recognition by a polymorphic cell surface receptor governs cooperative behaviors in bacteria. PLoS Genet. *9*, e1003891.
70. Pathak, D.T., Wei, X., Bucuvalas, A., Haft, D.H., Gerloff, D.L., and Wall, D. (2012). Cell contact-dependent outer membrane exchange in myxobacteria: genetic determinants and mechanism. PLoS Genet. *8*, e1002626.
71. Rousset, F., and Roze, D. (2007). Constraints on the origin and maintenance of genetic kin recognition. Evolution *61*, 2320–2330.
72. Crozier, R.H. (1986). Genetic clonal recognition abilities in marine invertebrates must be maintained by selection for something else. Evolution *40*, 1100–1101.
73. Jansen, V.A., and van Baalen, M. (2006). Altruism through beard chromodynamics. Nature *440*, 663–666.
74. Lyons, N.A., Kraigher, B., Stefanic, P., Mandic-Mulec, I., and Kolter, R. (2016). A combinatorial kin discrimination system in Bacillus subtilis. Curr. Biol. *26*, 733–742.
75. Wenren, L.M., Sullivan, N.L., Cardarelli, L., Septer, A.N., and Gibbs, K.A. (2013). Two independent pathways for self-recognition in Proteus mirabilis are linked by type VI-dependent export. MBio *4*, e00374-13.
76. Espinosa, A., and Paz-Y-Miño-C, G. (2014). Evidence of taxa-, clone-, and kin-discrimination in protists: ecological and evolutionary implications. Evol. Ecol. *28*, 1019–1029.
77. Yamazaki, K., Boyse, E.A., Miké, V., Thaler, H.T., Mathieson, B.J., Abbott, J., Boyse, J., Zayas, Z.A., and Thomas, L. (1976). Control of mating preferences in mice by genes in the major histocompatibility complex. J. Exp. Med. *144*, 1324–1335.
78. Manning, C.J., Wakeland, E.K., and Potts, W.K. (1992). Communal nesting patterns in mice implicate MHC genes in kin recognition. Nature *360*, 581–583.
79. Wedekind, C., Seebeck, T., Bettens, F., and Paepke, A.J. (1995). MHC-dependent mate preferences in humans. Proc. Biol. Sci. *260*, 245–249.
80. Takayama, S., and Isogai, A. (2005). Self-incompatibility in plants. Annu. Rev. Plant Biol. *56*, 467–489.
81. Brunet, T., and King, N. (2017). The origin of animal multicellularity and cell differentiation. Dev. Cell *43*, 124–140.
82. Janke, C., Magiera, M.M., Rathfelder, N., Taxis, C., Reber, S., Maekawa, H., Moreno-Borchart, A., Doenges, G., Schwob, E., Schiebel, E., and Knop, M. (2004). A versatile toolbox for PCR-based tagging of yeast genes: new fluorescent proteins, more markers and promoter substitution cassettes. Yeast *21*, 947–962.
83. Schindelin, J., Arganda-Carreras, I., Frise, E., Kaynig, V., Longair, M., Pietzsch, T., Preibisch, S., Rueden, C., Saalfeld, S., Schmid, B., et al. (2012). Fiji: an open-source platform for biological-image analysis. Nat. Methods *9*, 676–682.
84. Jacob, S., McClintock, M.K., Zelano, B., and Ober, C. (2002). Paternally inherited HLA alleles are associated with women's choice of male odor. Nat. Genet. *30*, 175–179.
85. Soares, E.V., and Mota, M. (1997). Quantification of yeast flocculation. J. Inst. Brew. *103*, 93–98.
86. Bayly, J.C., Douglas, L.M., Pretorius, I.S., Bauer, F.F., and Dranginis, A.M. (2005). Characteristics of Flo11-dependent flocculation in Saccharomyces cerevisiae. FEMS Yeast Res. *5*, 1151–1156.
87. Govender, P., Domingo, J.L., Bester, M.C., Pretorius, I.S., and Bauer, F.F. (2008). Controlled expression of the dominant flocculation genes FLO1, FLO5, and FLO11 in Saccharomyces cerevisiae. Appl. Environ. Microbiol. *74*, 6041–6052.
88. Di Gianvito, P., Tesnière, C., Suzzi, G., Blondin, B., and Tofalo, R. (2017). FLO5 gene controls flocculation phenotype and adhesive properties in a Saccharomyces cerevisiae sparkling wine strain. Sci. Rep. *7*, 10786.
89. Hope, E.A., Amorosi, C.J., Miller, A.W., Dang, K., Heil, C.S., and Dunham, M.J. (2017). Experimental evolution reveals favored adaptive routes to cell aggregation in yeast. Genetics *206*, 1153–1167.
90. Gillespie, D.T. (1977). Exact stochastic simulation of coupled chemical reactions. J. Phys. Chem. *81*, 2340–2361.

STAR★METHODS

KEY RESOURCES TABLE

REAGENT or RESOURCE	SOURCE	IDENTIFIER
Experimental Models: Organisms/Strains		
See Table S1 for list of strains	This study	
Oligonucleotides		
5′CAAAGAAATCTATAGGACCAAA AAC GGTGTTAATACAATCcg tacgctgcaggtcgac3′ Fwd primer for deletion of *ACE2*	This study	ace2mx_F
5′ATTATTTACTATGTTAATATCAT GCATA GATAAATGTTCGatc gatgaattcgagctcg3′ Rev primer for deletion of *ACE2*	This study	ace2mx_R
5′-ACTGCACAGAACAAAAA CCTGCAGGAA ACGAAGAT AAATCGAATTCGAGCTCGT TTAAAC-3′ Fwd primer for deletion of *URA3* to replace with GAL1p-*FLO1*	This study	ura3::FLO1_F
5′GTGAGTTTAGTATACAT GCATTTACTTATAATACAGT TTT tgaaagtatggaggagaaacag3′ Rev primer for deletion of *URA3* to replace with GAL1p-*FLO1*	This study	ura3::FLO1_R_2
5′CCGAGCAGAAGGAAGAACGA3′ Fwd primer to diagnose GAL1p-*FLO1* insert	This study	ura3::FLO1_dia_F
5′TGCCTCGGTGAGTTTTCTCC3′ Rev primer to diagnose GAL1p-*FLO1* insert	This study	ura3::FLO1_dia_R
5′ AACTGCTAATTATAGAGA GATATCACAG AGTTACTCACTAgg tcgacggatccccgggtt3′ Fwd primer to delete *LYS2* and replace with red or green fluorescent marker	This study	LYS2::TEF_GFP_F
5′ TAATTATTGTACAT GGACATATCATACGT AATGCTCAACCtcga tgaattcgagctcgtt3′ Rev primer to delete *LYS2* and replace with red or green fluorescent marker	This study	LYS2::TEF_GFP_R
Recombinant DNA		
pFA6-hphNT1	[82]	Euroscarf
pFA6a-TEF2Pr-eGFP-ADH1-Primer-NATMX4		N/A
pFA6a-TEF2Pr-dTomato-ADH1-Primer-NATMX4		N/A
Software and Algorithms		
JMP Statistical Software from SAS	SAS	https://www.jmp.com/en_gb/software/data-analysis-software.html
Fiji	[83]	N/A

RESOURCE AVAILABILITY

Lead Contact

Further information and requests for resources and reagents should be directed to and will be fulfilled by the Lead Contact, William Ratcliff (william.ratcliff@biology.gatech.edu).

Materials Availability

This study did not generate new unique reagents.

Data and code availability

The raw data supporting the conclusions of this manuscript will be made available by the authors upon request. The code analyzing microscopy images generating data for Figure 5 is available at Github (https://github.com/jenntpentz/Pentzetal2020_biomass_measurement).

EXPERIMENTAL MODEL AND SUBJECT DETAILS

All strains used in this study are listed in Table S1. We constructed snowflake and flocculating genotypes from a single clone of the initially unicellular *S. cerevisiae* strain Y55. Snowflake yeast were made as in [78], but we replaced the ACE2 ORF with HYGMX. Flocculating yeast were made by amplifying the KAN-GAL1p::FLO1 cassette from DNA template from *S. cerevisiae* strain KV210 [79, 80] and replacing the URA3 ORF in our ancestral strain. ura3Δ::KAN-GAL1p::FLO1/ura3Δ::KAN-GAL1p::FLO1 diploids were obtained by autodiploidization of single spores collected via tetrad dissection onto Yeast Peptone Dextrose plates (YPD; per liter: 20 g dextrose, 20 g peptone, 10 g yeast extract, 15 g agarose) then replica plated onto YPD + 200 mg/L G418. Transformants were confirmed by PCR as well as phenotype when grown in YPGal medium (per liter: 20 g galactose, 20 g peptone, 10 g yeast extract). For microscopy and competition experiments, strains were tagged with green and red fluorophores. To do this, plasmids pFA6a-TEF2Pr-eGFP-ADH1-Primer-NATMX4 and pFA6a-TEF2Pr-dTomato-ADH1-Primer-NATMX4 were amplified and inserted into the LYS2 locus, and transformants were confirmed via fluorescent microscopy. All transformations were done using the LiAc/SS-DNA/PEG method of transformation [84].

METHOD DETAILS

Measuring settling rate

Unlike snowflake yeast, floc yeast form groups as they are settling, so we needed to measure the properties of flocs during the process of settling directly. To do this, we developed a novel, robust, high-throughput method of measuring the settling speed of yeast populations. Various methods to measure aggregation and settling in yeast exist [24, 85–88], but most of them introduce experimental variables that limit their relevance to our system [85], and no method is considered standard in yeast research in general [85, 88, 89]. Importantly, most of them lack the temporal resolution needed (seconds) to capture the fast-settling profiles of some of our strains. In our method, we placed the yeast in back-illuminated cuvettes, and used high-speed high-resolution video acquisition (24 fps, 3840 × 2160 pixels, Sony a7R II, 90 mm macro lens) to capture changes in pixel densities over the settling time (Figures 1B and 1C). Our method relies in the fact that settling and flocculation produce optically denser regions, relative to the initial density distribution (Video S1), thus allowing us to measure the rate of this density changes. We pre-processed our raw density data with a Savitzky-Golay smoothing function in order to preserve the signal over the noise without sensibly changing the shape of the dynamics (Figures 1C and S6A). We then calculated a characteristic settling rate, as the maximum slope in the density dynamics. We validated our method by quantifying the percentage of biomass settled at 5 min in floc and snowflake cultures, showing that, as expected, a higher settling rate indicate a higher proportion of settled cells (Figure S6B).

Competitive success assay

To determine if snowflake yeast had a competitive advantage over floc yeast, we competed snowflake and floc starting at a range of initial genotypic frequencies (0%–100% snowflake in 10% increments) over two days of daily selection for fast settling for 5 min on the bench as in Ratcliff et al., 2012 [51]. We varied initial genotypic frequencies by changing the ratio of initial inoculum volume (e.g., a 50:50 ratio of snowflake:floc would have equal volumes of stationary phase cultures in the starting inoculum). To initiate competitions, we grew up snowflake and flocculating yeast in a mixture of galactose and glucose (YPGal+Dex; per liter; 18 g galactose, 2 g dextrose, 20 peptone, 10 g yeast extract) for 24 h at 30°C, shaking at 250 rpm. This concentration of galactose and glucose was used because it yielded clusters of similar size after 24 h of growth in snowflake and floc yeast (mean floc log(volume) = 12.5, mean snowflake log(volume) = 11.5, $t(2) = -0.39$, $p = 0.73$). Then, we mixed five replicates of 500 μL of each starting genotypic frequency from overnight cultures and 100 μL of this culture was diluted into 10 mL YPGal+Dex for the competition experiment. We used the remaining 400 μL to measure the initial count of snowflake and floc yeast. To do this, we used EDTA (50 mM, pH 7) to deflocculate cells to run through a CyFlow® Cube8 flow cytometer where two distinct peaks corresponding to unicellular floc cells and snowflake cultures could be counted. Then, we measured the change in frequency of snowflake yeast over the course of the experiment by flow cytometry. Specifically, we deflocculated flocs with EDTA (which does not affect group affect group size in snowflake yeast), and then

measured their cell number density (cells / mL) and the number of snowflake yeast clusters (clusters / mL). Because the distribution of snowflake yeast cluster sizes is stable in these short-term experiments, we can calculate the change in ratio between floc cells and snowflake clusters across the experiment, and infer the change in strain frequencies. We measured the number of unicellular floc and snowflake yeast after inoculation but before any growth and after three days of competition. We calculated the competitive success of snowflake yeast as the ratio of snowflake to floc yeast after competition relative to before competition using the Equation (1):

$$\text{Competitive success} = \frac{f_2(1-f_1)}{f_1(1-f_2)} \quad \text{(Equation 1)}$$

where f_1 is the frequency of snowflake yeast before competition and f_2 is the frequency of snowflake yeast after competition [43]. This fitness measure is simple and general (i.e., it doesn't assume any underlying model of population dynamics, like exponential growth), and accommodates different starting frequencies.

Invasion from rare experiment

To determine if snowflake and floc yeast stably coexist when they constitute 80% of the population, we ran a longer competition experiment. To start the competition, we grew floc and snowflake yeast in YPGal+Dex for 24 h at 30°C, shaking at 250 rpm. Next, we mixed overnight cultures of floc and snowflake yeast at a 2.5:97.5 floc:snowflake initial inoculum ratio (t0 on Figure 3E). We inoculated a 10 mL culture of fresh media with 100 μl of the mixed culture (t1) with 5 independent replicates. Everyday, after 24 hours of growth, we transferred 1.5 mL of each culture into eppendorf tubes, and applied 5 minutes settling selection on bench top. After 5 minutes, we discarded the top 1.4 mL and transferred the remaining bottom 100 μL into a fresh 10 mL culture. In total, we applied 10 rounds of settling selection.

To measure the daily fraction of both genotypes, prior to the settling selection, we first de-flocculated the floc yeast by pelleting and resuspending in 1 mL of overnight culture in 50 mM EDTA. Next, we vortexed cultures for 10 s and pipetted 10 μL of each replicate onto microscope slides. Finally, we imaged each microscope slide using the bright field channel on a Nikon Eclipse Ti inverted microscope at 100x magnification. We ensured all cells on the microscope slide were imaged by combining 81 separate images images (9x9 composite image). We saved each frame as individual TIFF files (81 frames x 11 time points x 5 replicates), then inspected each frame for their quality and deleted frames of images with large air bubbles. Then, we ran an ImageJ Marcro script to automatically count the number of floc and snowflake yeast clusters. Next, we removed all tiny dirt particles by applying an 'awk' one-liner on Bash (Unix) by removing particles that were smaller than the size of single cells, which corresponded to the 'arbitrary unit' of 400 (a.u.) in our images. To assign particles as floc or snowflake yeast, we first detected the minimum 'arbitrary unit' (a.u.) size for the smallest snowflake yeast clusters given by the ImageJ Macro. As a result, we assigned particles that are between 500-3000 (a.u.) as floc yeast and particles that were larger than 3000 (a.u.) as snowflake yeast. We validated these size-based thresholding parameters manually for each sample at every time point. When calculating the fraction of snowflake yeast in mixtures of floc and snowflake yeast populations, we counted every single snowflake yeast cluster as 'one' single individual regardless of their cluster size, and measured the fraction of snowflake yeast for each day (11 days in total).

Competitive success during growth and settling

There are two important life history traits in our experimental system: growth rate and settling rate [51, 53]. We measured the competitive success of snowflake yeast during both stages. To do this, we grew snowflake and floc yeast separately for 24 h in YPGal+Dex. As above, we mixed five replicates of 500 μL of various starting genotypic frequencies (10%–90% snowflake in 20% increments) from overnight cultures and we used 100 μL to dilute into fresh YPGal+Dex and used the remaining 400 μL to calculate initial snowflake and unicellular floc counts as described above. To measure snowflake competitiveness during growth, we deflocculated 500 μL of each culture using EDTA and measured snowflake and floc counts using flow cytometry after 24 h of growth at 30°C, shaking at 250 rpm. To measure competitive success over one round of settling selection, we aliquoted 2 mL of each snowflake/floc co-culture into 2 mL microcentrifuge tubes. Next, we aliquoted 500 μL into 1 mL microcentrifuge tubes and deflocculated to obtain pre-selection snowflake and floc concentrations as described above. We allowed the remaining 1.5 mL to settle on the bench for 5 min, after which the top 1.4 mL was discarded. Finally, we deflocculated the remaining 100 μL and obtained post-selection snowflake and floc counts via flow cytometry.

Examining aggregate composition

We measured the composition of snowflake and floc yeast within large chimeras by fluorescent microscopy, using a Nikon Eclipse Ti inverted microscope with a computer-controlled Prior stage. Specifically, we grew up snowflake and floc-GFP for 24 h in YPGal+Dex. Next, we mixed four replicates of snowflake and floc co-cultures with differing amounts of starting snowflake (20% or 80%, respectively) into fresh medium and grew these co-cultures for another 24 h. We placed 10 μL of this culture between a slide and a 25 × 25 mm coverslip and imaged the whole coverslip by combining 150 separate images at 100 × magnification, yielding a 42456 × 42100 pixel (1.78 billion pixels; 1.23 × 1.22 cm) composite image. To determine the per pixel area of each genotype in all yeast clusters within the composite image (including yeast cell 'clusters' of size 1), we used a custom Fiji Macro script [83]. Then, we calculated the percentage of biomass in different cluster size classes belonging to either snowflake or floc yeast using a custom Python script. Briefly, we first binned all yeast clusters into 10 cluster size classes. Then, we calculated the frequency of floc and snowflake yeast within each cluster size class using the per pixel areas determined using Fiji. This script has been made available at GitHub (see Data and Code Availability for details). "Large flocs" were considered to be anything larger than the largest snowflake clusters (Figure 5C).

Mathematical modeling

We consider a settling competition between snowflake clusters and flocculating cells. If flocculation, settling, and reproduction all occur together we might expect a complicated set of dynamics resulting from the interplay between these processes. We simplify our analyses by focusing strictly on aggregation. We assume that aggregation and settling happen after the primary growth phase and occur faster than reproduction such that the populations of cells are large as a result of several generations of reproduction in media. Furthermore, we consider aggregation and settling selection as two separate processes such that there is some time in which cells aggregate and afterward the groups are exposed to settling selection. This assumption allows us to focus on modeling the dynamics of aggregation and circumvent explicit spatial models that would be required to consider the dynamic interactions between aggregation and settling. Based on these assumptions, we model the dynamics of aggregation using a system of differential equations, where the concentration of snowflake clusters composed of i cells is denoted as S_i, flocs of i choosy cells is denoted as C_i, and permissive flocs of size i is denoted as P_i. (see Equations 2, 3, 4, and 5). Because our model considers a fixed volume, concentrations are proportional to population size.

The equation for flocs of i choosy cels (Equation 2) relates the difference in concentration of C_i to the difference between two terms. The first term counts the ways that two smaller choosy cell flocs can bind to give rise to a floc of size i. The second term counts the ways a floc of size i can bind to other flocs, thereby forming larger flocs that are no longer size i. The $\delta_{i,j}$ term is a delta function that accounts for the extra loss if two identically-sized flocs interact, i.e., if two C_i bind then the loss is double that of a C_i binding a C_j where $i \neq j$.

$$\frac{dC_i}{dt} = \sum_{j=1}^{\frac{i}{2}} p(i-j,j)C_jC_{(i-j)} - \sum_{j=1}^{N-i} p(i,j)(1 + \delta_{i,j})C_iC_j \qquad \text{(Equation 2)}$$

Since the number of differential equations scales with the maximum floc size, we assume thatthere is a maximum size N (N = 1000 in our computations) for numerical tractability. In addition, we choose a time for the aggregation process such that the concentration of flocs of maximum size is small in comparison to the total concentration. Because we are modeling the process of aggregation alone, we also note that our model ignores the possibility of group fragmentation, i.e., flocs can bind to form larger flocs but not break up into smaller flocs.

An influential component of Equation 2 is $p(i,j)$ which describes the rate that flocs of choosy cells bind to form larger flocs, i.e., $C_i + C_j \rightarrow C_{i+j}$, where $i + j \leq N$. The actual rate function $p(i,j)$ likely depends on many factors including the geometry of the two flocs, the probability of collision, the probability of a collision resulting in binding, etc.. We assume that it is a simple function of the radii of the two flocs: $p(i,j) = \beta\,(r_i + r_j)^3$ where β is a rate constant and r_i and r_j are the radii of C_i and C_j that result from approximating the flocs as spheres. Thus, if the volume of a single cell is $\frac{4}{3}\pi r^3$, then the volume of C_i is $(i)\frac{4}{3}\pi r^3$ which makes the radius of C_i equal to $i^{1/3}r$. We consider $r = 1$ to simply the calculations. As a result the probability function $p(i,j)$ has the form $p(i,j) = (i^{1/3} + j^{1/3})^3$.

The equations describing the aggregation dynamics of permissive flocs and snowflake clusters are similar to those used for choosy flocs but with the feature that snowflake cells and permissive cells can bind. To allow for this provision, we use P_i to denote permissive flocs which contain permissive cells and possibly snowflake cells. Thus, a P_i cluster may be composed of k permissive cells and $i - k$ snowflake cells for any $k \geq 1$. In contrast, S_i denotes a group of only snowflake cells. Equations 3 and 4 describe the changes in concentrations of permissive flocs and snowflake cell clusters that result from permissive flocs binding each other as well as snowflake clusters.

$$\frac{dP_i}{dt} = \sum_{j=1}^{i-1} p(j,i-j)S_jP_{i-j} + \sum_{j=1}^{\frac{i}{2}} p(j,i-j)P_jP_{(i-j)} - \sum_{j=1}^{N-i} p(i,j)P_iS_j - \sum_{j=1}^{N-i} p(i,j)(1 + \delta_{i,j})P_iP_j \qquad \text{(Equation 3)}$$

$$\frac{dS_i}{dt} = -\sum_{j=1}^{N-i} p(i,j)S_iP_j \qquad \text{(Equation 4)}$$

For our calculations we want to track the concentrations of snowflake cells both within snowflake clusters and permissive flocs. Since the differential equation approach is based on concentrations of cells, we assume that there are a large number of both clusters and cells and track the concentration of snowflake cells in P_i clusters for each size i, which we denote n_i. This assumption corresponds to treating the aggregative mixture as a classic tank mixing problem. As a result, the total concentration of snowflake cells is $\sum_{i=1}^{N}(i\,S_i + n_i)$.

$$\frac{dn_i}{dt} = \sum_{j=1}^{i-1} p(j,i-j)S_jP_{i-j}\left(j + \frac{n_{i-j}}{P_{i-j}}\right) + \sum_{j=1}^{floor\left(\frac{i}{2}\right)} p(j,i-j)P_jP_{i-j}\left(\frac{n_j}{P_j} + \frac{n_{i-j}}{P_{i-j}}\right) - \sum_{j=1}^{N-i} p(i,j)P_iS_j\left(\frac{n_i}{P_i}\right) - \sum_{j=1}^{N-i} p(i,j)(1 + \delta_{i,j})P_iP_j\left(\frac{n_i}{P_i}\right)$$

(Equation 5)

In all competitions except for Figures S3 and S4, we assume an initial inoculum of 1000 concentration units that is split between C, S, and P. The initial distribution of S_i is fit to a lognormal distribution that matches empirical data (Figure S3A). This distribution only changes in the presence of permissive floc. The winner of the settling competition is determined by solving Equations (2, 3, 4,

and 5) for some time t and selecting the largest 10% of the population, using group size as a proxy for settling speed. This is analogous to our experimental system, where 10% of fastest-settling yeast biomass gets passaged to the next tube following settling selection. For C cells, as time increases, more of the distribution is represented in the largest fractions ($\approx i = N$; Figures S2C and S2D). Thus, the amount of C cells in the top 10% of possible clusters size increases with time, but levels out for longer t (Figure S2D).

The mathematical model captures a single round of aggregation and selection without regard to how populations grow in between selective events. In cases where we consider multiple rounds of aggregation and selection (Figures S3H and S3I), we do not use any explicit models of population growth. Rather, we multiply the final proportions of cells after selection by the inoculum size and use that as the input to the next iteration of aggregation and selection. This bypasses the possibility that different population growth dynamics might alter the proportions of cell types. In addition, we also assume that the P and S cells dissociate from their mixed groups and begin the next aggregation and selection phase as separate entities. We also consider a stochastic model for aggregation described below that does not require a limit to the maximum group size nor large numbers of clusters and cells. Figure S5 shows that its results agree with the deterministic differential equations model.

Stochastic model

To further verify the findings of our deterministic model, we consider an alternative stochastic model. The model has the same qualitative features in that there are three types of cells: choosy (C), snowflake (S), and permissive (P). As with the deterministic model, choosy cells can only form clusters with themselves while permissive cells can form clusters with themselves or with snowflakes. We use a Gillespie algorithm approach [90] with the reaction scheme shown below. C_n denotes a choosy floc of n cells, P_n is a permissive floc of n cells, S_n is a snowflake cluster of n cells, and $SP_{(n,m)}$ is a floc with n snowflake cells and m permissive cells. The binding rates are the same as those found in the deterministic model such that $p(i,j) = \beta(i^{1/3} + j^{1/3})^3$.

$$C_i + C_j \xrightarrow{p(i,j)} C_{i+j} \quad \text{(Equation 6)}$$

$$P_i + P_j \xrightarrow{p(i,j)} P_{i+j} \quad \text{(Equation 7)}$$

$$S_i + P_j \xrightarrow{p(i,j)} SP_{i,j} \quad \text{(Equation 8)}$$

$$SP_{i,j} + P_k \xrightarrow{p(i+j,k)} SP_{i,j+k} \quad \text{(Equation 9)}$$

$$SP_{i,j} + S_k \xrightarrow{p(i+j,k)} SP_{i+k,j} \quad \text{(Equation 10)}$$

$$SP_{i,j} + SP_{k,l} \xrightarrow{p(i+j,k+l)} SP_{i+k,\ j+l} \quad \text{(Equation 11)}$$

We simulate the aggregation dynamics using the Gillespie algorithm [90] which involves repeated iterations of determining when the next reaction occurs and which reaction it is. Both decisions require calculating the reaction propensity for each reaction. The reaction propensity of a specific reaction is simply the product of the number of combinations of substrates and the reaction constant. For example, the reaction propensity of two choosy flocs of size i and j binding is the product of the number of C_i flocs, the number of C_j flocs, and $p(i,j)$. After calculating the reaction propensity for every reaction, we determine the time for the next reaction by sampling from an exponential distribution with a mean of 1/X, where X is the sum of all reaction propensities. We determine which reaction occurs by transforming the reaction propensities into probabilities; this can be done by dividing each reaction propensity by X. We assign each reaction a unique range of values within [0,1], sample a random number from a uniform distribution over [0,1], and then choose the matching reaction. Thus, if the probability of two choosy flocs of size i and j binding is 0.01, then the reaction may have the range of values [0,0.01] and will only occur if the random number sampled is within this range. Once a reaction is chosen we modify the number of reactants of each type and repeat the process until there are no more reactions to occur or a specified time has occurred.

We simulate the aggregate dynamics using this stochastic approach for 100,000 cells until no more aggregation events can occur, which usually occurs around time = 0.1, although the value depends on the scaling of $p(i,j)$. In simulations with only choosy cells, the flocs do not reach sizes comparable to snowflake clusters until some time between 0.005 and 0.02. Thus, we choose a time of 0.01 and show the same type of plots as displayed in Figures 6A–6C in which there are pairwise competitions of the various cell types and the largest 10% of clusters are selected (Figure S5). The initial distribution of snowflake clusters follows the same exponential distribution as used in the deterministic equations.

The results confirm the original findings of our deterministic approach in which snowflake cells have an advantage over permissive cells for all initial proportions while the outcomes of competitions involving choosy cells depend on the initial proportions (Figure S5).

Direct measurement of settled biomass

To validate our imaging-based approach for quantifying settling speed, we measured biomass settling for floc and snowflake yeast directly. We grew five replicates of floc or snowflake yeast in 10 mL YPGal+Dex for 24 h at 30°C, shaking at 250 rpm. Then we placed 1.5 mL of stationary-phase cultures in a pre-weighed 2 mL microcentrifuge tube. We allowed yeast to settle for 5 min at 1 × *g*, after which we transferred the top 1.4 mL to a different pre-weighed tube. After this, we pelleted and double-washed yeast with deionized water, then we removed the excess water and the pellet was airdried 50°C for two days. We determined the settling rate as the percentage of total biomass in the bottom 100μL pellet.

Measuring the ratio of FLO+ and FLO- unicells in flocs

We measured the ratio of flocculating (*FLO1*) and non-flocculating (*flo1*) cells in flocs to determine of *flo1* cells are preferentially excluded. We grew *FLO1*-GFP and *flo1* cells separately for 24 h in YPGal+Dex. Then, we mixed three replicates of *FLO1*-GFP and *flo1* cocultures with a starting ratio of 90:10 *FLO1*-GFP: *flo1* or 50:50 *FLO1*-GFP: *flo1*, and inoculated 100 μL of these co-cultures into fresh medium and grew them for another 24 hours. We separated flocs from planktonic cells and deflocculated the flocs with EDTA. We measured the number of cells of each type in the floc and planktonic populations via flow cytometry.

Measuring the frequency of dead cells

We measured the rate of dead cells in 'floc' and 'snowflake' yeast by growing six biological replicates of each genotype. Both strains were grown in 10 mL of liquid YPGal+Dex cultures for 24 hours at 30°C, shaking at 250 rpm. Next, we diluted each strain 1:100 into fresh YPGal+Dex cultures and grew them for 12 hours at 30°C, shaking at 250 rpm. We then pipetted 1 mL of all 12 samples into 1.5 mL microcentrifuge tubes, pelleted them, discarded the liquid media and washed them in 1 mL sterile water. Next, we incubated the yeast with the red dead-cell stain propidium iodide (PI) for 5 minutes (in 1:1000 dilution of 1mg/ml PI stock solution). After the incubation period, we centrifuged and washed the cells in sterile water. To measure the fraction of dead cells, we imaged them on a Nikon Eclipse Ti inverted microscope. Briefly, we imaged 6 replicates of each strain at 100x magnification by taking 4x4 frames of images under both bright field and red fluorescence (FITC) channels. We measured the number of total individual cells using bright field images. To measure the number of dead cells, we merged red and bright field channels using Fiji [83] and counted the number of red cells. Finally, we calculated the fraction of dead cells in each sample.

QUANTIFICATION AND STATISTICAL ANALYSIS

Standard statistical analyses were performed using JMP statistical analysis software (https://www.jmp.com/en_us/home.html). Student's t test and ANOVA with post hoc Tukey honestly significant difference (HSD) test were performed where $p < 0.05$ was considered statistically significant. See Results and figure legends for the statistical details.